Facile Handling of 3D Two-Photon Polymerized Microstructures by Ultra-Conformable Freestanding Polymeric Membranes

Hoed, Frank Marco den; Ottomaniello, Andrea; Tricinci, Omar; Ceseracciu, Luca; Carlotti, Marco; Raffa, Patrizio; Mattoli, Virgilio

Published in:
Advanced Functional Materials

DOI:
10.1002/adfm.202214409

Publication date:
2023

ADVANCED FUNCTIONAL MATERIALS
www.afm-journal.de

Facile Handling of 3D Two-Photon Polymerized Microstructures by Ultra-Conformable Freestanding Polymeric Membranes

*Frank Marco den Hoed, Andrea Ottomaniello, Omar Tricinci, Luca Ceseracciu, Marco Carlotti, Patrizio Raffa, and Virgilio Mattoli**

Micro-nano-fabrication on objects with complex surfaces is essential for the development of technologies in the growing fields of flexible electronics and photonics. Various strategies are devised to extend the fabrication from conventional planar substrates to curved ones, however, significant challenges still exist, especially in the framework of 3D printing and additive manufacturing. In this study, a novel technique is presented to realize 3D micro-structures on arbitrary complex surfaces providing an extreme level of conformability. This method relies on the fabrication of micro-structures via two-photon polymerization on polymeric nano-membranes that can be efficiently transferred to a specific target. Ultra-thin polymeric films are exploited as the support to suspend and transfer the printed micro-structures on the predefined surface. The nanofilm can finally be easily removed, apart from the region underneath the printed elements where it serves as a few tens of nanometers adhesive. The repeatability and feasibility of the proposed process are investigated and shown to provide large flexibility of choice on the printed structures, materials used, transfer procedures, and targeted substrate geometries. By integration with standard fabrication processes, the described technique offers a great potential for the development of next-generation multidimensional/multi-material micro-nano-technologies.

1. Introduction

The past decades were marked by a growing interest in the development of novel micro-fabrication methods that allowed the incredible technological breakthroughs of our time. This combined effort of academia and industry resulted in a rapid increase of our fabrication capabilities in terms of resolution, scalability, throughput, and geometrical/structural complexity of the realized micro-nano structures. However, these conventional techniques rely on traditional types of lithography, such as photo- and electron-beam lithography, and (one-photon) direct laser writing, which are inherently 2D, and, as such, limited to fabrication only on flat and extended surfaces.

Nano- and micro-fabrication of arbitrary structures directly on morphologically complex surfaces is essential for the design and fabrication of devices that have to be employed in applications such as flexible electronics,[1,2] photonics,[3,4] and micro-electromechanical systems (MEMS).[5,6]

The fundamental idea behind conformal fabrication methods has gained traction in the last decades, finding its origin from flexible and wearable electronics.[7,8] The developed techniques in this framework allow the direct fabrication of functional devices on non-flat substrates, such as curved[9] and stencil lithography,[10,11] electro-hydrodynamic lithography,[12] 3D printing,[13] laser-induced hydrothermal growth,[14] self-assembly,[15] and laser direct writing.[16–18]

In this setting, direct laser writing (DLW) enabled by two-photon polymerization (2PP) processes offers a great potential to realize arbitrary 3D micro-structures with submicrometric resolution and high precision.[19–21] Its integration with other methods and its possible exploitation on arbitrary complex systems can significantly improve applicability, thereby opening up unprecedented opportunities for the fabrication of highly conformable multifunctional devices for sensing, imaging, and communication. However, this is seldom explored in the scientific literature and most of the examples of DLW by 2PP are confined to work on planar substrate. To the best of our knowledge, only very few demonstrations of printing on unconventional

F. M. den Hoed, A. Ottomaniello, O. Tricinci, M. Carlotti, V. Mattoli
Center for Materials Interfaces
Istituto Italiano di Tecnologia
Via R. Piaggio 34, Pontedera 56025, Italy
E-mail: virgilio.mattoli@iit.it

F. M. den Hoed, P. Raffa
Smart and Sustainable Polymeric Products, Engineering, and Technology institute Groningen (ENTEG)
University of Groningen
Nijenborgh 4, Groningen 4747 AG, The Netherlands

L. Ceseracciu
Materials Characterization Facility
Istituto Italiano di Tecnologia
Via Morego, 30, Genova 16163, Italy

The ORCID identification number(s) for the author(s) of this article can be found under https://doi.org/10.1002/adfm.202214409.

DOI: 10.1002/adfm.202214409

targets have been achieved, such as the fabrication on a cylindrical surface[22,23] or tip of optical fibers[24,25] in the framework of micro-optics.[26] In all cases, the 2PP printing is limited to simple structures or requires a complex procedure for the preparation of the substrate or the customization of the 2PP set-up. A straightforward and fully versatile method to realize full 3D micro-structures while maintaining the performance of state-of-the-art 2PP DLW is therefore highly demanded.

A promising approach to achieve this objective consists of the use of conformable substrates. The exploitation of flexible materials, both as the substrate or/and the support to transfer or stamp the fabricated devices in an effective and versatile way, allows to realize transistors,[27] LEDs[28] and energy harvesting devices,[29] solar cells[30] and conformable sensors,[31,32] just to name a few. Although a transfer or stamp introduces an additional step to the fabrication process, thereby increasing effort and reducing process reliability compared to direct fabrication, the processes are non-invasive and straightforward. At the same time, fine conformability and wrapping on rough and curved surfaces are only possible with transfer printing, while established fabrication technologies cannot accomplish similar complexity, versatility, and printing resolution. In this regard, different strategies for transfer printing have been devised according to the specific targeted application, which can include the use of soft[33] or bio-inspired adhesives,[34] in-plane structures on sacrificial layers[35,36] and ultra-thin membranes.[37,38] The latter, which provides the lowest possible achievable thickness, represents the ideal support to obtain the highest physical contact with the targeted surface. As the bending stiffness of the material cubically depends on its thickness, ultra-thin films are characterized by strongly enhanced flexibility guaranteeing an extreme level of conformability and adhesiveness to arbitrary curved objects.

In this work, we developed a novel method that allows an efficient transfer characterized by extreme conformability of 2PP-printed micro-structures by employing ultra-thin polymeric films as printing substrates, with the aim to extend the range of applicability of 2PP printing to non-standard surfaces.

By printing directly on a few tens of nanometers thick poly(vinyl formal) (PVF) layer able to spontaneously delaminate in water from a rigid substrate, 3D microstructures can be straightforwardly handled and transferred on an arbitrary final target. The nano-membrane thus serves two functions as an ultra-thin support for the microstructures and as a conformable layer to perfectly adhere, through van der Waals interaction, to complex interfaces. In the final step, the layer can be conveniently removed to provide only a nanometers thick adhesive for the transferred elements.

We investigated the feasibility and reproducibility of the method, by suspending arrays of micro-structures of arbitrary shape with large flexibility of single-element aspect ratio, filling factor, and array surface extension (up to tens of millimeter squares). Additionally, we developed two different transfer techniques, defined as air- and water transfer, which allow to achieve an unprecedented degree of conformability and procedural flexibility. We show several demonstrations of the potential of the proposed technique for the integration of 2PP micro-structures on targets with completely non-standard surfaces. Among all, these include the placement of a micro-element on the tip of a 30 µm wide cantilever via air-transfer, and the all-around conformal wrapping of a metallic wire of 12 µm radius with an array of 3 µm size micro-structures.

The proposed 2PP on nanofilms method could thus open new perspectives in micro-nano-technology by extending 2PP-printing to non-conventional interfaces, as well as other micro-fabrication techniques.

2. Transfer Printing of 2PP 3D-Microstructures via Nanomembranes

In the perspective of constructing 3D conformal structures on curved/complex surfaces, transfer printing methods constitute the most convenient and efficient process. The possibility to obtain complex designs or devices performing planar lithography which can be subsequently transferred on a specific substrate can provide superior fabrication capabilities in terms of efficiency, quality, stability, and cost-effectiveness with respect to performing the 3D-printing directly on the targeted interface. In the approach we are describing, we combined the superior 3D-microprinting performances offered by DLW with an advanced transfer printing method based on freestanding ultrathin nano-membranes (only previously demonstrated on 2D structures), thus resulting in an effective route for the realization of complex and high aspect ratio 3D micro-structures on arbitrary surfaces. Examples of ultra-thin polymeric films (with thickness < 1 µm) comprise a variety of applications that span the fields of polymer science,[39] biomedics,[40] tissue engineering,[41,42] sensing,[43] and, more recently, wearable/flexible electronics[44–46] and photonics.[28,47] Accordingly, in these latter demonstrations, polymeric nano-films were used as free-standing supports to achieve device adhesion on nonplanar surfaces owing to their few nanometer thicknesses, which maximizes the adhesion by dispersion forces and minimize the strain forces originating from bending phenomena (which might induce damage). This is because, for a thin plate, as the film thickness (t) decreases the bending stiffness of the film (D), given by the product of the film Young's modulus (E) and the second-moment area (I), approximately varies according to Equation 1:[27,35]

$$D = E \cdot I = E \frac{t^3}{12\left(1-\nu^2\right)} \tag{1}$$

where ν is the film Poisson ratio. This equation states that the degree of conformability of a film can increase significantly by reducing its thickness, independently from its intrinsic elasticity. Typically, a thickness below 1 µm results in film self-adhesion to an arbitrary 3D surface due to Van der Waals interactions, avoiding the need of additional adhesive agents.

Various methods to realize ultra-thin free-standing polymeric film has been developed, which most commonly consist of the film deposition on a substrate, its release, and suspension on support. Each of these processes has to deal with the limiting factor represented by the increase of the strain (ε, which cannot be arbitrarily high) required for film delamination from the substrate as the film becomes thinner, which progressively hampers the achievement of an arbitrary thin layer thickness.

A thickness threshold for film delamination is in fact defined by Equation 2:[48]

$$t = 2\frac{1+\nu}{1-\nu}\frac{\Delta\gamma}{E\cdot\varepsilon^2} \quad (2)$$

where $\Delta\gamma$ is the difference in interfacial energy between the laminated and delaminated state of the film. Moreover, as the film thickness decreases below 1 µm, the direct peeling from the substrate is impractical due to the difficulty in keeping a uniform strain field during peeling to not detrimentally affect the film properties, especially in the case of large area films or/and without the use of a supporting overlayer. It is possible to circumvent these limitations by employing a sacrificial layer between the film and the substrate which can be dissolved selectively thus allowing the nanofilm to release and be captured freestanding on a final support. This methodology allowed the realization of nanofilms with thickness of tens of nm on areas of cm-scale linear size (i.e., aspect ratio of 10^6) and able to hold up weight 70.000 times their own mass.[35] However, achieving lower thicknesses or/and larger surfaces with this technique is limited due to the challenging deposition of extremely smooth and uniform sacrificial layer, which otherwise creates defects affecting the mechanical properties of the final suspended film. Interestingly, another approach was developed to directly lower the delamination threshold in water.[48] This relies on the substrate functionalization with a polyelectrolyte, polydiallyldimethylammonium (PDAC), which shows limited affinity toward a specific polymer, poly(vinyl formal) (PVF), while increasing the hydrophilicity of the substrate, thus resulting in the spontaneous delamination enhancement of the PVF film when the system is slowly immersed in water. Layer thicknesses as low as 8 nm, aspect ratios as high as 10^7,the bearing of loads 10^6 times the film mass,[48] and conformability to bending radii lower than 1 µm have been achieved[45] with this method. Even though this method is suitable and can be applied to other polymers,[48] the large-scale fabrication of high mechanical robustness homogeneous nanomembranes made of PVF reveals this polymeric material as the best candidate to achieve high throughput and versatile transfer printing via ultra-thin films. Here we in fact demonstrate that we can extend this approach from the 2D domain to the 3D one with high repeatability and reproducibility by exploiting PVF nanomembranes. In the developed method PVF nanofilms served both as support for the transfer of 3D micro-structures and as a few tens nanometers-thick adhesive to conform them to morphologically complex planar and non-planar interfaces. The fabrication procedure can be subdivided into four main steps (as summarized in **Figure 1**a): PVF nanofilm preparation, delamination, planar 2PP micro-structures printing, and transfer on the final target. First, a silicon wafer substrate was spin-coated with the cationic polyelectrolyte PDAC, baked, rinsed accurately with water, and dried to form only a strongly bound sub-nanometric functionalization which guarantees the spontaneous release of the film in water (following the procedures reported by Baxamusa et al.[48]). A PVF solution in ethyl lactate was then spin-coated to obtain a few nanometers thick polymer film. Several thicknesses (25–100 nm) could be prepared by varying the PVF concentration (film thickness calibration curves in Figure S1, Supporting Information). The as-prepared wafer was then employed as substrate to directly perform 2PP of micro-structures with standard printing parameters and a commercial photoresist, which can be photopolymerized in DiLL (Dip-in laser lithography) configuration (i.e., lens immersion mode). The edges of the film area to be delaminated were defined on the spin-coated wafer using a cutter blade. The wafer sample was then immersed in a deionized water bath at ≈45° angle to achieve the direct delamination of the selected film area carrying the 3D printed micro-structures, which can float on the water surface.

As a final step, the transfer on the predefined final target can be performed. According to the specific application, two options are possible: the direct collection of the film with the printing from water using the final target itself, or the suspension of the film on a suitable holed frame to transfer the printing by air on the substrate in a second moment.

Images during the fabrication steps for representative 2PP micro-structures arrangements are reported in Figure 1 for both types of transfer. Figures 1b,c,d show an array of 5 µm diameter, 10 µm high pillars array after 2PP printing, suspended via the PVF film on a circular frame and finally transferred on another flat substrate through air, respectively. The transfer process is achieved by simply approaching by hand until contacting the bottom interface of the nanofilm with that of the substrate.

These preliminary tests indicated the feasibility of the whole process, highlighting the following observations: the ability of the PVF film to still easily delaminate after the printing step of the micro-structures (i.e., the PVF was not affected by a standard 2PP printing process), the preservation of the film's mechanical properties and flatness upon suspension (see Figure 1e for an example of high aspect ratio freestanding elements), the perfect conformability of the film on the final substrate, thus the adhesion with preservation of the initial microstructures arrangement on the targeted surface. Remarkably, after the transfer process, treatment with oxygen plasma can remove the PVF layer everywhere apart from the surface underneath the 2PP elements where the 50 nm thin PVF acts as an adhesive layer via van der Waals interaction with the second interface (as further discussed in following sections). Importantly, this etching process does not affect any feature of the performed 3D printing (as verified by profilometer measurements shown in Figure S2, Supporting Information). Moreover, the transferred structures were tested to be resistant to standard 2PP cleaning processes in solvents like acetone or isopropyl alcohol for at least 30 min at room temperature. In Figure 1f, we show an example of the feasibility of the transfer performed directly from water. In this case, the transfer is performed by immersing the object in water underneath the film and collecting it on top while moving it out from the water bath. The synergic combination of water surface tension and van der Waals forces provided a very good conformability of a high filling factor array of 1 µm diameter pillars on a smooth but high curvature edge (≈2 µm bending radius) of a piece of PDMS specimen cut with a surgical blade. Oxygen plasma cleaning removed the nanofilm but did not affect the adhesion of the pillars. Other examples of transferred 2PP structures, with high filling factors or complex 3D shapes, are reported in supporting information (see Figures S3 and S4, Supporting Information).

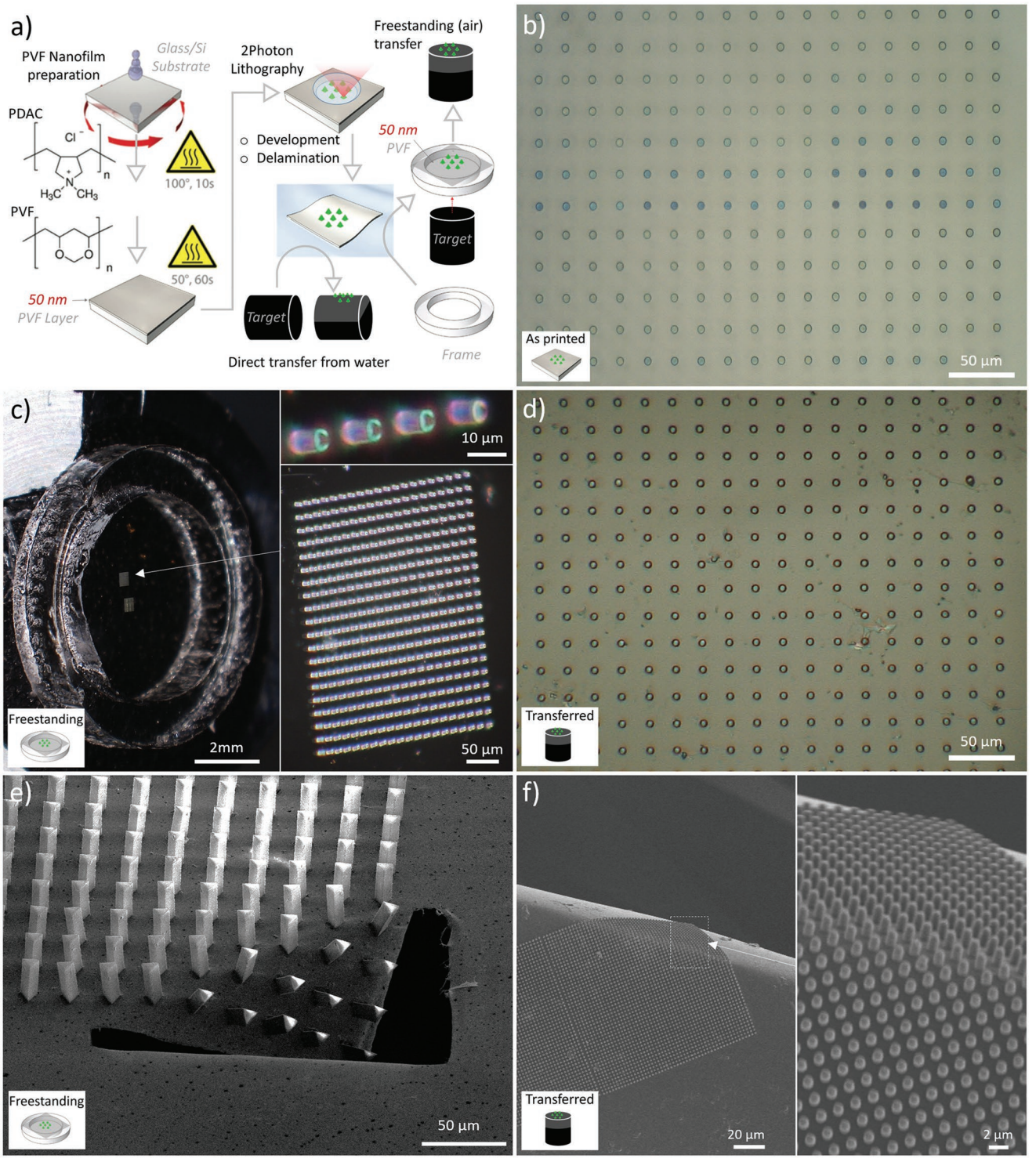

Figure 1. a) Steps of the fabrication technique of 2PP-printed microstructures on complex surfaces. Optical images of the stages of a representative sample during fabrication: b) square array of 5 µm-diameter pillars after 2PP printing on a PVF spin-coated silicon wafer, c) free-standing 2PP structures after delamination and suspension of the 50 nm thick PVF film on a holed frame. Insets: zoom on the printed micro-pillars at increasing magnification. d) Air-transferred array on a flat substrate after oxygen-plasma cleaning to remove PVF film residues. e) SEM image of high aspect-ratio (10 µm lateral size, 30 µm high)-structures free-standing on a PVF film. A focused-ion beam etching has been performed to highlight the suspension of the structure. f) SEM image of a high filling factor array of 1 µm-diameter pillar directly transferred from water on the edge of a cut PDMS specimen (bending radius of the edge ≈2 µm).

Interestingly, the two transfer methods are not identical but each offers some key advantages that the other does not, and thus they can be seen as complementary. In particular, air transfer is more versatile as it can allow to create directly free-standing devices, but also their controlled handling and high precision positioning onto the final target. On the other hand, water transfer, thanks to water surface tension, permits higher conformability and adhesion, at the expense of a lower alignment flexibility, as discussed in the following. All details of the fabrication procedure, including both types of transfer, are then reported in Section 4.

2.1. Systematic Investigation of the Method Feasibility

In order to study the feasibility, reproducibility, and possible limitations of the proposed technique, we performed a systematic investigation of the dependence of the delamination and the transfer printing on the main parameters characterizing the process, film thickness, DLW printing parameters, geometrical parameters of the structures. Initially, we identified the thickness of the PVF layer which guarantees the best compromise between film robustness to handle the structures throughout the entire process and the highest possible conformability. This means aiming for the highest possible thickness where mechanical re-delamination from the target substrate after transfer is still impossible and thus ensuring good adhesion. Equation 2 provides a theoretical prediction of this optimum considering the limit strain (strain at failure) as the strain ε. Theoretical estimation has also been directly validated by performing scratch tests on films transferred to silicon wafers, as detailed in the supporting Figure S5 (Supporting Information), both indicating as optimal a PVF film thickness of 50 nm which has been consistently kept constant for all described processes.

The DLW printing process showed no detrimental influence on the delamination and the mechanical properties of the PVF layer. We tested different commercial photoresins (IP-Dip, IP-L, and IP-S) and found that the procedure was successful regardless of the material and the printing parameters (laser power ranging from 20 to 40 mW, and laser speeds from 10.000 to 20.000 μm s^{-1} depending on the used photoresin). It is worth mentioning that we did not need to modify the standard printing parameters when employing the spin-coated polymer rather than the bare silicon wafer. To develop the process, however, we focused mostly on the use of IP-Dip due to its improved resolution compared to other resists of the IP Series while maintaining similar mechanical properties (Young's modulus of a few GPa). Moreover, IP-Dip allows the largest possible range of applications, such as in microoptics, micromechanics/MEMS, and integrated photonics.

We then explored the effect on the transfer of the geometric parameters of the printed structures, such as shape, aspect ratio, and filling factor. Square arrays of 3D microstructures with planar bases with basic shapes (triangular, square, and circular) were printed varying their interdistance/periodicity and aspect ratio (i.e., height to in-plane linear size ratio). A summary of the printed structures after performing a transfer in air on another planar silicon wafer is shown in **Figure 2** (and the complete set tested is reported in Figure S6, Supporting Information). All the transfers we performed were successful regardless of the tested parameter ranges (aspect ratios from 0.5 to 5 and filling factor up to ≈70%), hinting to little effect of the geometry of the structures and their unit cell on the delamination and transfer yields. Moreover, the limit of highest possible filling factor (i.e., a uniform extended structure) was tested to be successful; such as the delamination and transfer of a 3 × 3 mm^2 2PP square with a few micrometers thickness (shown in Figure S7, Supporting Information). This realization thus enlarges the range of applicability of the proposed method even to printed structures with an arbitrary high filling factor. Regarding the aspect ratio, the study was limited to a reasonable range for standard applications of this kind of micro-structure arrangements, while taking into account the final goal to achieve a high degree of conformability to the largest possible range of targetable complex/curved surfaces. Other examples to highlight the performance of the developed technique can be found in Supporting Information (see Figure S8, Supporting Information). Notably, all performed processes were successfully finalized throughout the explored parameters range, which therefore does not represent the ultimate limit range for the micro-structures geometric parameters targetable by the proposed technique. The minimum size of single transferable elements is ultimately limited by the 2PP printing resolution, while the maximum dimension (both planar and out-of-plane) is only constrained by the geometric features of the targeted surface (overall size, curvature, or local morphology in general) for the transfer. Accordingly, the realization of conformal transfer of several cm^2 2PP structures was obtained, as shown in Figure S9 (Supporting Information). Furthermore, both large-scale nanofilm preparation techniques[48] and feasible large-scale nanofilm transfer from the water surface[49] enable the application of the proposed 2PP printing handling method to on-demand surface areas.

2.2. Precise Air-Transfer Alignment of 2PP Structures on Complex Surfaces

We then tested the feasibility of the transfer on complex morphology targets and surfaces, first performing it after film suspension and final transfer through air. A PVF film carrying the 2PP printed structure was suspended on a ring-shaped holder to be transferred on a non-conventional substrate. For this step, 2 mm thick plastic holders with an internal hole diameter of 2 cm were standardly used. The 2PP printed structure was approximately centered on the frame by hand to have the widest range of in-plane movement to perform the precise transfer on the final target. In this case, the dimension of the latter was limited by the holder hole diameter, but the suspended area can be straightforwardly extended to several cm^2 as already demonstrated.[44,48] In order to control with micrometer precision the positioning of the microstructures, the holder was then fixed to a three-axis motorized stage having both tuneable step-size and motion speed in the 0.5–10 μm and 1–200 μm s^{-1} range, respectively. The apparatus was mounted close to an optical microscope (HRX-01 3D digital microscope from Hirox) to perform imaging of the sample while performing the transfer procedure. By placing the predefined target underneath the holder

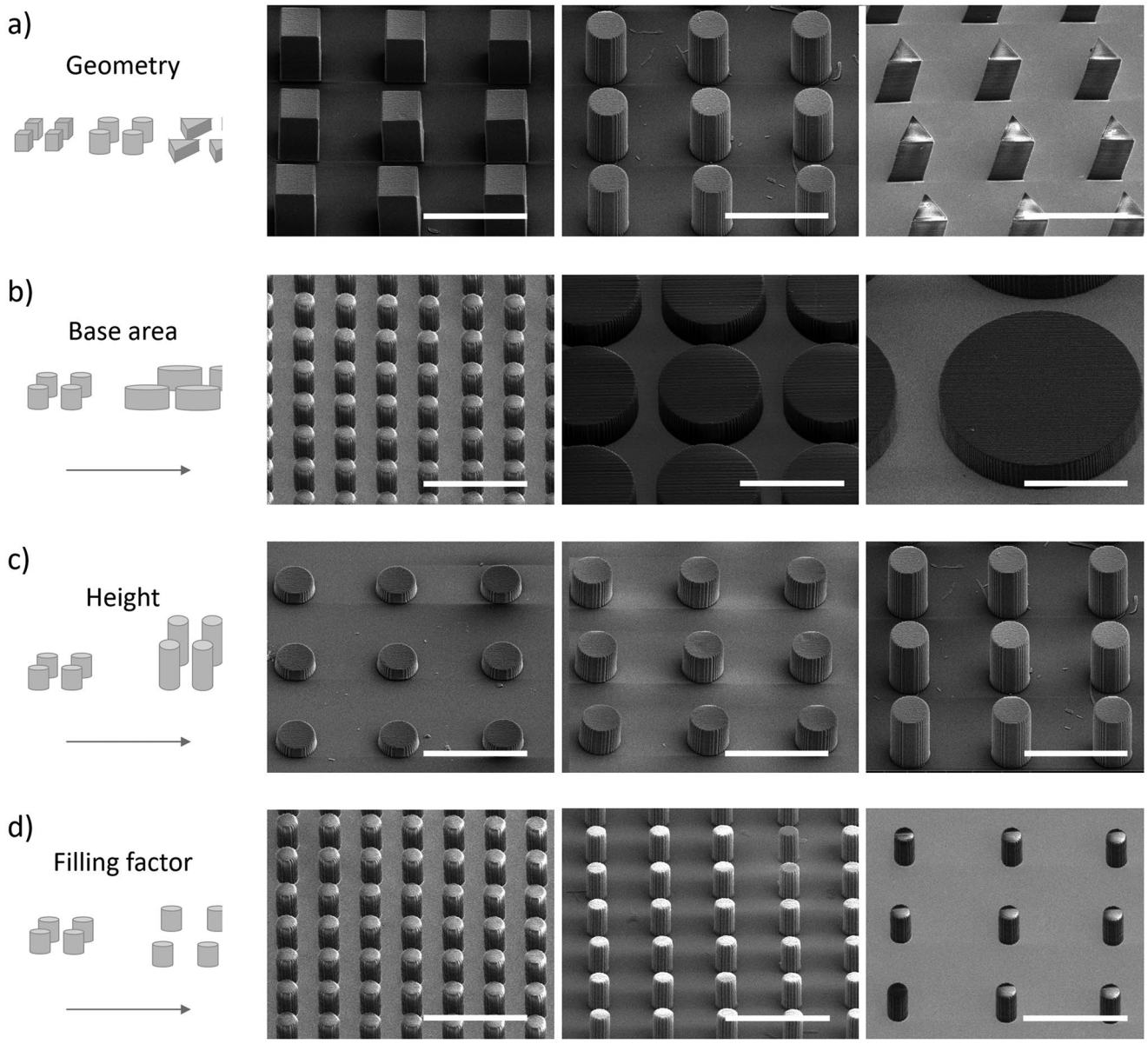

Figure 2. Systematic investigation of the transfer technique feasibility depending on the geometric parameters of the 2PP printed micro-structures: unit-cell geometry, aspect ratio, and filling factor. a) SEM images of square arrays of 2PP printed micro-structures with different geometries (parallelepipeds with square and triangular bases, and pillars). b) For a fixed geometry (pillars), the base area is changed while the height (10 µm) and gap distance (5 µm) between elements are fixed. Three different pillar diameters are reported by optical images: 5, 25, and 50 µm (from left to right). c) SEM images of pillar arrays with a fixed pillar radius (10 µm) and gap distance (15 µm), but different heights (5, 10, and 15 µm). d) Optical images with pillar arrays with different gap distances (5, 10, and 20 µm) and fixed pillar diameter (5 µm) and height (10 µm). Images have the same magnification, the scale bar fixed to 25 µm is common to all the images. All the SEM images refer to structures after release and air-transfer on a planar silicon substrate, by means of 50 nm thin PVF film. Nevertheless, film thicknesses in the range between 25 and 100 nm showed as well successful transfer printing but provided less reproducibility.

as shown in **Figure 3**a, the full transparency of the film allowed to finely align the 2PP elements on a precise location on the target. Using the mid-range objective allowing magnification in between x140 and x1000, both vertical and in-plane relative displacement between the printed structures and the target surface could be easily identified. Figure 3b shows the 2PP structures during the alignment and transfer procedure on the target, a 30 µm wide atomic force microscope cantilever.

By moving the PVF film toward the cantilever with µ-steps, the in-plane alignment was progressively optimized until contact when the nanofilm could be observed to adhere to the cantilever surface. Further increasing the height of the holder, a sufficient strain is generated to tear the film and release the microstructures on the target. van der Waals interactions allowed the 2PP element to conform and adhere to the cantilever during transfer and remain in place even after the

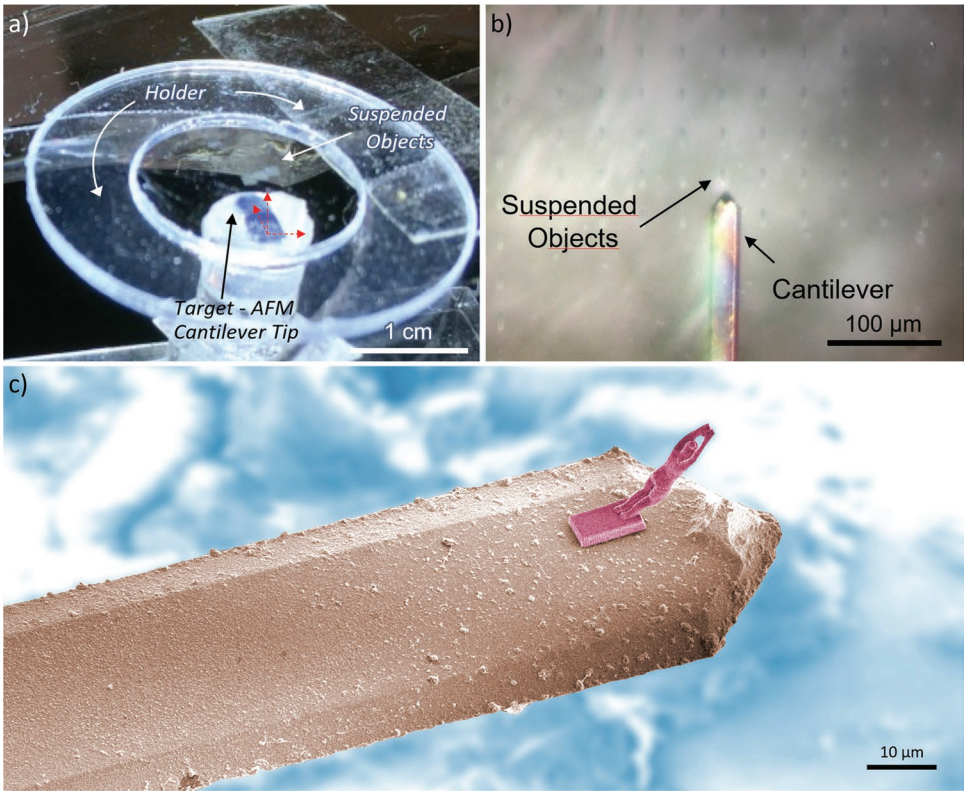

Figure 3. Air-transfer of 2PP-printed micro-structures on a non-standard target. a) Image of a free-standing PVF nano-membrane carrying 2PP objects to be transferred on the underneath target (i.e., an atomic-force microscope cantilever tip). b) High-precision alignment of the suspended micro-structures on the final target performed using an optical microscope and x-y-z stages for target positioning. c) Final result of the air-transfer procedure. A single 30 µm-high, 5 µm-width elements (i.e., 2PP-printed "diver") is placed with micrometric precision on the front edge of a cantilever tip. This transfer demonstrated the ability of the developed method to transfer with micrometric precision an arbitrary 3D micro-structure on a non-standard substrate presenting complex edges, which is not as easily targetable by standard fabrication procedures.

removal of the PVF residues, as shown in Figure 3c. Using the described procedure and set-up, the described air-transfer method was demonstrated to reproducibly achieve micrometer precision aligned transfer on top of non-standard flat but also curved surfaces (as also shown in Figures S10 and S11, Supporting Information). Higher alignment precision can eventually be targeted by exploiting piezo-driven stages and providing appropriate isolation from background vibrations.

2.3. Transfer of 2PP Micro-Structures on High Curvature Interfaces and Complex Surfaces

We also explored the potential of the proposed method to conform 3D micro-structures on highly curved surfaces by taking advantage of the capillary forces generated during a transfer in water. For this purpose, a specific holder is used to transfer a PVF film supporting the 2PP elements on the lateral surface of a 25 µm diameter wire.

The direct collection step on the holder of the delaminated PVF film carrying the microstructures floating on the water surface and its transfer on the wire are shown in **Figure 4**a,b. The latter is suspended in such a way as to create a 4 mm gap with the bottom of the holder. This gap is fundamental to avoid the PVF film to wrap multiple times on the wire surface during collection by the adhesion of film tails on the holder ground. After drying, the PVF film could be removed using oxygen-plasma etching as described earlier, thus obtaining the all-around conformability of the printed array of micro-cones on the cylindrical surface of the wire, as shown in Figure 4c,d. Also in this case very good adhesion is guaranteed by the van der Waals interaction of the polymer with the surface, while the water surface tension provided a sufficient strain on the film to make it perfectly conform to the substrate.

This demonstration reveals the suitability of the proposed technique to achieve perfect conformability of 3D printed structures on extremely small radius of curvature by exploiting the described water transfer. Interestingly, this process can enable the realization of highly conformable ultra-thin optical devices by 2PP with great potential for application in the emerging field of flexible and integrated photonics.[47] This application shows that the developed technique is also suitable for the conformal transfer of metalized micro-structures, which extends its applicability to create freestanding highly conformable devices with a hybrid composition of plasmonic and dielectric structures.

In order to test the full potential of this approach, we also employed the transfer methodology, performed both in water and in air, on surfaces that presented both a high curvature and a complex morphology. For example, in **Figure 5**a we show an array of micro-prism that was transferred through water on the

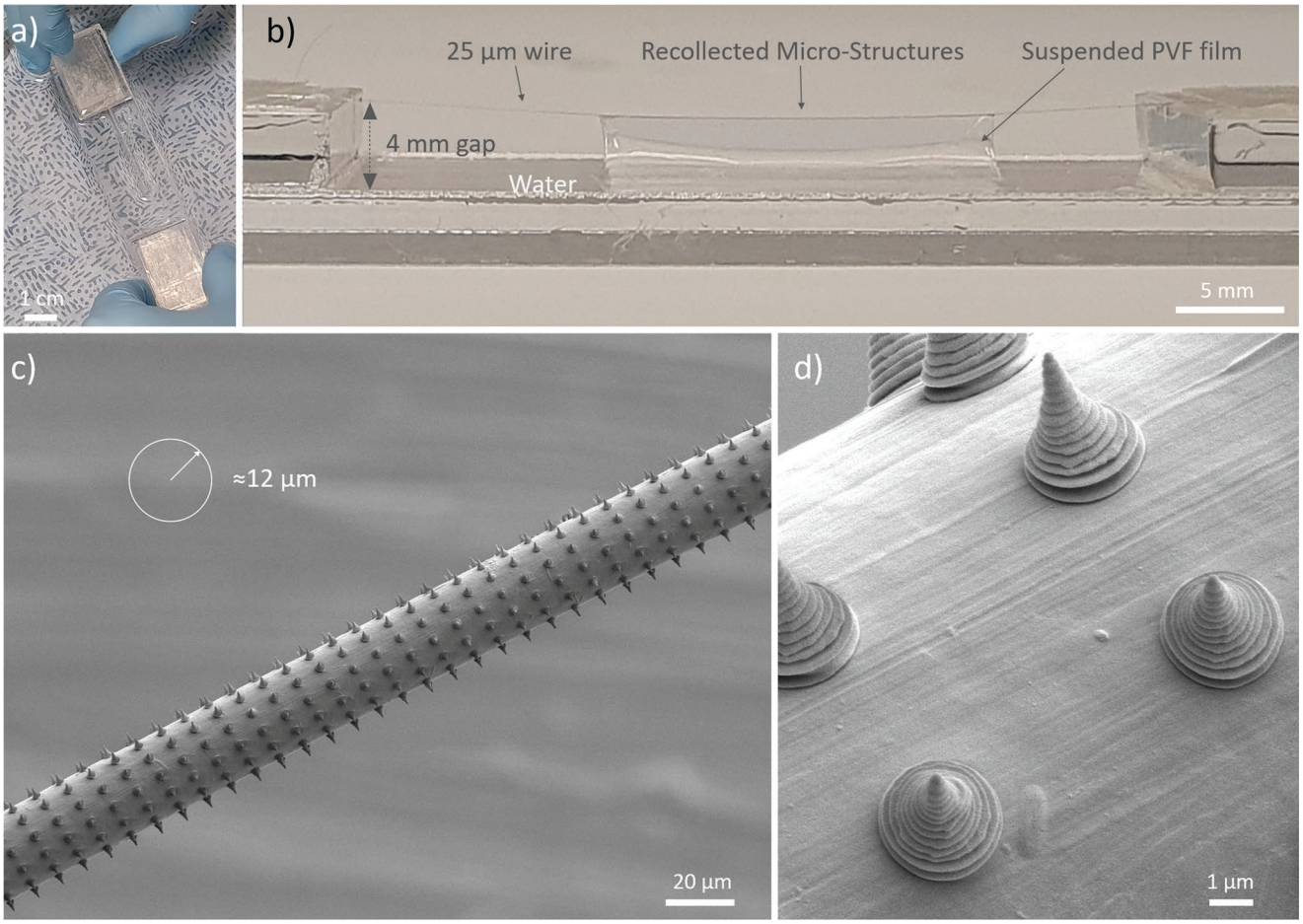

Figure 4. Water-transfer of 2PP-printed micro-structures on a high curvature target. a) Direct collection from the water of a delaminated PVF nanofilm carrying the 2PP print on a metal wire suspended on a specific holder. b) Optical image of the collected membrane adhering on the suspended metal wire after the collection step. c,d) SEM images of the all-around conformed 2PP-printed micro-elements (i.e., array of 3 µm-size cones) on a µm-radius metal wire after oxygen-plasma removal of the PVF nanomembrane exploited for the transfer. Bare micro-structures can be observed to adhere to the high curvature wire surface.

irregular interface of a human hair (45 µm-radius). The array can be observed to show 360° conformability independently of the surface roughness of the hair (see Figure 5b).

The possibility of achieving an excellent adhesion of 2PP printed elements on arbitrary complex targets is also shown in Figure 5c,d. Here, 3D micro-structures were transferred on the multi-curved surface of a gold fragment exploiting the air transfer method described in Section 2.2.

The performed demonstrations thus show the broad applicability and reproducibility of the technique to obtain conformal transfer on highly curved but also morphologically irregular and multi-oriented surfaces, as also additionally reported in (see Figures S12 and S13, Supporting Information).

A distinction between possible targetable surfaces highlights the advantages and performance limitations of the developed transfer techniques. Focusing on developable surfaces, as arbitrarily small bending radii can be targeted by water transfer, the limitation of conformability is dictated by the size (both thickness and in-plane dimension) of the transferred micro-structures depending on the specific curvature/application, and ultimately by the 2PP printing resolution. In the case of non-developable substrate surfaces (non-zero Gaussian curvature), the first constraint is still the specific size of the micro-structures, and finally the limited stretchability of the exploited polymeric membranes. However, owing to the nanofilms to microstructures thickness ratio investigated in this work, the latter factor has only a negligible contribution, which may only matter at a sub-micrometer level. A major limiting factor that nanofilm transfer through air can encounter is to conform on high aspect ratio cavities due to a combination of strain induced by adjacent already adhered surfaces, plus air trapping. This can be to some extent circumvented by water transfer thanks to the capillary effect which can force adhesion on otherwise not accessible cavities after drying.

As a general description, water transfer provides higher transfer flexibility and conformability performance with respect to air transfer, at the expense of reduced alignment precision which can be achieved by user handling for relatively large dimensions of printed structures (enough extension to be identified by eyes on the water surface). Air transfer on the other hand provides the possibility to achieve high precision alignment even of a small/single structure on the same range of

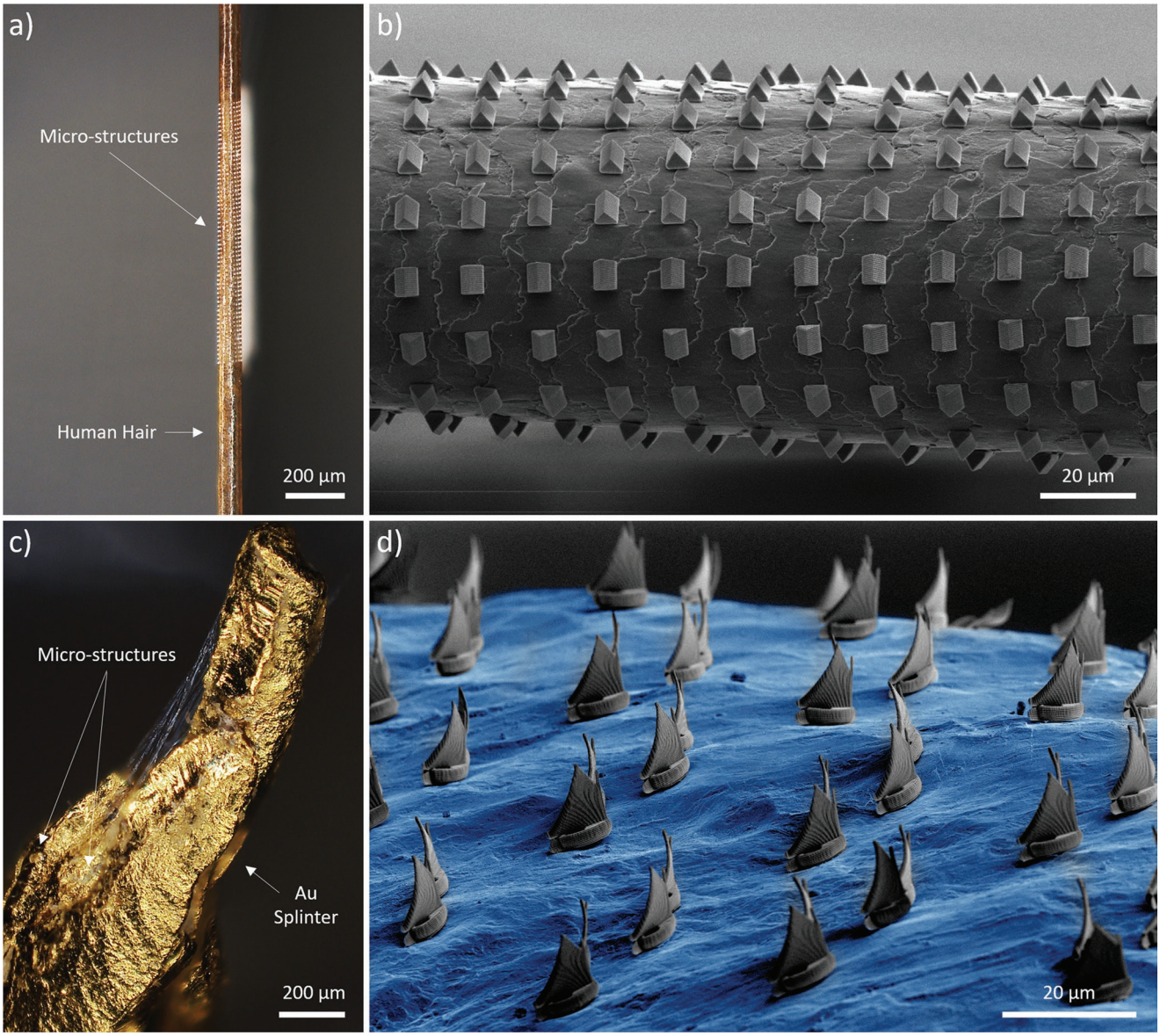

Figure 5. Demonstrations of transfer on arbitrary complex and curved surfaces. a) A 45 µm-radius human hair wrapped by 2PP-printed micro-structures transferred from water. b) SEM image of the conformal transfer of the printed array around the specific target. c) Gold fragment with 2PP-structures transferred in air. d) SEM image of the transferred elements (i.e., 2PP "sail-boats") on the complex surface of the specific target.

possible targets, but with some limitation in terms of conformability (as impracticable perfect all-around conformability). The combination of the two techniques can achieve a compromise between alignment and adhesion performance; as obtained by performing the same steps of the air transfer procedure, but on a previously wet surface, as shown in Figure S13 (Supporting Information).

2.4. Adhesion Test of 2PP Micro-Structures

The PVF thin layer underneath the transferred 2PP structures provides their physical contact and glue-free adhesion via van der Waals interactions with the final substrate. The few tens of nanometers thickness guarantee a very low flexural rigidity which enhances the conformability by increasing the contact area of the film with the target surface. Accordingly, both adhesion force and critical load for polymeric film delamination have been reported to rapidly increase as the film thickness lowers below a few hundred nanometers, easily achieving values higher than 105 N m^{-1} and 10 µJ cm^{-2},[50] respectively.

Nevertheless, in our case, the adhesion of the micro-structures on the final surface depends on both the microstructures-film and film-substrate interfacial interactions. We thus designed and performed experiments to test the effective adhesion strength of the 2PP structures upon transfer on the final target. Several identical samples consisting of a square array of 30 µm diameter, 40 µm high pillars were prepared with the

developed technique and transferred through air on the flat surface of glass substrates. Other duplicates of the same structures were instead printed directly on the bare glass surface of identical substrates as reference. First, the micro-structures adhesion was tested against substrate actuation. The samples were in fact directly mounted on a loudspeaker. This was used to apply a sinusoidal and square wave acceleration to the microstructures. The produced acceleration was simultaneously detected by an integrated three-axis accelerometer. Both transferred and reference structures were not affected by actuating up to ± 53 g acceleration in all three directions with oscillation frequencies spanning from a few Hz to hundreds of kHz (see also Figure S14, Supporting Information). This observation thus revealed the robustness of the transferred samples at least to vibrations that can be experienced in lab or real-world environments.

In order to further investigate the 2PP micro-structures adhesion, a second experiment was performed, which directly allowed the application of a load to the 2PP elements. The glass substrates were mounted on a 3D-printed holder to fit their dimension and to ensure their planarization. A customized cantilever (made of a polymide multilayer) was fixed to a load cell, and it was moved down from the vertical direction until contact with the glass surface of the samples by using a manual translation stage. A compact microscope was integrated into the setup in order to image the microstructure arrays in transmission from the back of the transparent glass substrate, allowing to align the arrays to the pre-loaded cantilever. The samples were then scanned in one direction using a motorized stage to obtain the direct contact of the cantilever with the 2PP structures, thus exerting a friction force on them (parallel to the scan direction), namely proportional to the preload. The load time evolution and its effect on the microstructures could thus have been acquired in real-time during scanning. The set-up details and image can be found in Section 4 and Figure S15 (Supporting Information), respectively. We tested reference samples and transferred microstructures (after plasma-oxygen cleaning). We estimated a threshold pre-load for the detachment of microstructures from the substrate of ≈3 ± 1 mN for the reference samples, while a 6 ± 1 mN in the case of transferred 2PP structures. The experiment thus revealed comparable, if not slightly higher adhesion forces, of the transferred structures with respect to those directly printed on the bare glass, as it is usually performed in 2PP printing. Finally, we considered as an additional step of the fabrication procedure the coating of the transferred 2PP microstructures with a parylene C layer with the aim of enhancing the adhesion/anchoring to the final substrate. Among other coatings, Parylene C constitutes an ideal choice for reinforcement of micro-structure elements, due to its high level of conformability (guaranteed by chemical vapor phase deposition), its excellent insulation properties, and to the precise deposition thickness controllability.[51] A 1 µm thick layer of parylene C was thus conformably deposited on the transferred samples with the aim to improve the robustness of the final structure to applied shear stresses. The contact load experiment was then repeated for the parylenized structures. Notably, in this case, no detachment of any micro-elements was observed from all tested samples up to the maximum applicable pre-load (18 ±3 mN), thus demonstrating the effectiveness of the parylene coating to strongly enhance the robustness of transferred elements. Complete test results are reported in Table S1 (Supporting Information).

Perfect adhesion of microstructures to the substrate and conformal coating of parylene was also subsequently verified by means of focused ion beam (FIB) cross sectioning, and SEM image on the parylene-coated sample once several sweep tests were repeated (see Figure S16, Supporting Information).

3. Conclusions

There is a high demand for efficient and reliable conformable fabrication methods to integrate micro-nano-technology with complex surfaces in a plethora of different fields. In this work, we addressed the possibility of extending 3D microprinting via two-photon polymerization from planar substrates to complex 3D surfaces presenting arbitrary morphologies. There are only limited examples in the literature of additive manufacturing that target these objectives despite the fact that such techniques could dramatically broaden the scope of 2PP and offer novel integration possibilities with other established micro-nano fabrication techniques.

The innovative methodology we propose relies on the exploitation of nanomembranes made of PVF as both a flexible substrate for the printing and a sacrificial support to handle and transfer 2PP micro-structures on a predefined arbitrary substrate. After delamination in water, the nanomembrane can in fact be directly collected on the final target or suspended on a specific holder to be transferred through air with high precision. At the end of the transfer process, the excess of nanofilm apart from the region underneath the printed elements can be selectively removed by using an oxygen plasma descum. We first performed a systematic investigation of the nanofilm delamination behavior upon immersion in water while carrying the 2PP elements, and testing for the printing parameters, material used, and geometry of the realized structures. A thickness of 50 nm was identified as the ideal compromise between robustness of the film during the process, conformability performance, and ease of its removal. Finally, a large flexibility in the choice of the photoresin for the 2PP printing was observed.

We therefore performed a series of demonstrations in order to show the potential of the developed technique, exploiting two different transfer processes, defined as air- and water-transfer. The transfer through air was found to be particularly suitable to achieve high-precision placement of 2PP structures on non-standard complex substrates, while water transfer was revealed ideal for the conformal adhesion to high curvature interfaces. Employing these approaches, across the realized demonstrations, we highlight the placement of a micro-element on the tip of a 30 µm wide cantilever, the transfer of an array of high aspect ratio structures on the non-developable surface of a metal fragment, and the all-around wrapping of 3D objects on the surface of a 12 µm radius wire. Importantly, the developed technique was also demonstrated to be suitable for the integration of 2PP structures with metallic layers to provide the fabrication of hybrid plasmonic-dielectric optical devices for application in the emergent fields of flexible photonics and micro optical electro-mechanical systems.[47]

Both transfer techniques thus showed complementary performances and versatility to fabricate 3D micro-structures on completely non-conventional surfaces, which standard 3D printing methods or, in general, other state-of-the-art fabrication procedures cannot as easily achieve. Moreover, the adhesion strength of transferred microstructures was experimentally tested to reveal similar adhesion to standard 2PP printing performed on the same substrate. Notably, the microstructure encapsulation with just a 1 µm thin layer of parylene C is shown to guarantee strong enhancement of 2PP structure adhesion force to the final target.

Thanks to the inherently 3D-geometric flexibility, continuously improving resolution and availability of two-photon polymerizable functional materials, the proposed fabrication method shows great potential to serve not only as an independent technique to realize extremely conformable devices but also as a complementary procedure to elevate current state-of-the-art fabrication techniques to the fabrication of next-generation multimaterial/multi-dimensional micro-nano-technologies.

4. Experimental Section

Materials Used and Film Preparation: PVF (trade name Vinylec K), Ethyl lactate (EL, ≥ 98%, FCC, FG), and PDAC (20% wt. in water solution) were purchased from Sigma-Aldrich. These materials were used to perform spin-coating on the polished surface of 2 inches diameter (381 ± 25 µm-thick) silicon wafers by Silicon Materials (Si-Mat). A PDAC 0.5% wt solution in water was prepared by diluting the commercial 20% wt solution with MilliQ water. Such a solution was used to functionalize the Si wafers. After first for performing a plasma oxygen treatment to enhance the wettability of the wafers (60 W, 1 min), ≈2 mL PDAC solution was deposited and spin-coated at 4000 rpm for 15 s. The wafers were then baked at 100 °C for 10 s on a hotplate. By rinsing them with deionized water for a few seconds in order to dissolve the PDAC residues, the wafers are dried with a compressed air gun. A 1.5% wt. PVF solution in EL was prepared by dissolving the appropriate amount of PVF in 20 mL of EL. Solutions were stirred at 650 rpm at a temperature of 50 °C until all PVF was dissolved. PVF solutions were filtered immediately before use with a hydrophobic filter (0.2 µm pores diameter, Minisart). The PVF solution was then spin-coated over the PDAC sub-nm layer in a two-step process of a total duration of 10 s. During the first 5 s, spin-coating speed was set at 300 rpm while during the remaining 5 s it was set at 3000 rpm. About 2 mL PVF solution was deposited for each nanosheet spinning session and the substrates were then baked for 60 s at 50 °C on a hotplate. The PVF nanosheet thickness measurement was performed by means of a P-6 stylus profilometer (KLA Tencor, USA) averaging over 10 measured values randomly acquired on the film surface before the release from silicon-wafer. For the PVF concentration used the measured thickness was found equal to 50 ± 2 nm.

Microstructure 2PP Printing: Direct laser writing (DLW) of the dielectric structure of the device was performed by 2PP using the Photonic Professional GT-2 (from Nanoscribe) using the commercial 2PP photoresin IP-Dip (Nanoscribe) in DiLL configuration with a 63x objective. The PVF spin-coated silicon wafer provided a clear interface for the 2PP printing whose bottom plane was fixed at 0.5 µm underneath the silicon interface. For all the realized 2PP structures, the printing parameters were set to those suggested by the manufacturer (laser power: 20 mW; beam scanning velocity 10.000 µm s^{-1}. The slicing and hatching distance are fixed both at 0.3 µm. The development was performed in PEGMEA (8–10 min) followed by IPA rinsing (3 min) to carefully remove photoresin residues. Printing times up to 10 h were not observed to affect the mechanical properties of the nanofilm in terms of delamination and robustness. However, printing for a long time may create point defects that affect the delamination process, which we speculate could be caused by photoresin infiltration in between the PVF layer and silicon substrate.

Delamination Process: Before immersing in water the spin-coated substrate for delamination, we defined the PVF surface area to be delaminated by using a surgical blade. As a standard, a PVF surface of 15 × 15 mm^2 centering each printed set of structures was defined. The borders of the silicon wafer were also carved to ease the delamination process. Operatively, the delamination was performed by progressively immersing each silicon wafer in a DI water bath with a ≈45° angle at a speed that allows the film to spontaneously delaminate without creating excessive stress on the film (fraction of mm s^{-1}).

Film Suspension on Frame: Once the film was completely released and floating on the water surface it could be collected from the top via a specific holder by handling it with standard tweezers. As a standard, the holders were made of a holed PMMA frame with internal and external diameters spanning from 0.8–2 cm and 1.3–2.5 cm, respectively, and thickness of 2 mm. Once centered the frame on the region presenting the 2PP microstructures, the holder was approached until contact with the floating film, which was able to attach via van der Waals forces to the frame borders. During the pick-up rotational movement, the water tension allowed to perfectly flatten the film and ensured its adhesion on the frame. The film was then left under a hood until it was completely dried. The film can be eventually stored in vacuum or in an environment with low humidity until the final transfer; no deterioration of the film is observed even after a few months.

Scratch Tests: The tendency to delaminate of transferred films was characterized through scratch tests on an Anton Paar Micro-combi head, equipped with a Vickers tip. Contact load was the minimum allowed by the instrument, 30 mN, and from there was ramped up until 100 mN, while the stage was displaced perpendicularly to the applied load. The onset and type of damage were evaluated after each test with the built-in microscope.

Adhesion Test Setup and Details: The experimental apparatus to perform the measurements of 2PP microstructure adhesion test was composed of: a tension/compression load cell (model LRF400, from Futek Company) equipped with a customized polyimide cantilever, a linear motorized stage with repeatability to 0.1 µm (model L-509, from PI), a manual linear stage with standard micrometer (model PT1, from Thorlabs) and a commercial low-cost USB microscope. The measurement scanning with the motorized stage was performed at a speed of 10 µm s^{-1}. The measured load noise was ≈0.3 mN.

Supporting Information

Supporting Information is available from the Wiley Online Library or from the author.

Acknowledgements

F.D.H. and A.O. contributed equally to this work. The authors gratefully acknowledge support from the European Union's Horizon 2020 research and innovation program under the FET Open grant agreement 5DNanoPrinting-no. 899349.

Open access funding provided by Istituto Italiano di Tecnologia within the CRUI-CARE agreement.

Conflict of Interest

The authors declare no conflict of interest.

Data Availability Statement

The data that support the findings of this study are available from the corresponding author upon reasonable request.

Keywords

micro-electromechanical systems, microfabrication, nanofilms, transfer printing, two-photon polymerization

Received: December 9, 2022
Revised: February 21, 2023
Published online: March 22, 2023

[1] H. Zhou, W. Qin, Q. Yu, H. Cheng, X. Yu, H. Wu, *Nanomaterials* **2019**, *9*, 283.
[2] S. Cai, Z. Han, F. Wang, K. Zheng, Y. Cao, Y. Ma, X. Feng, *Sci. China Inf. Sci.* **2018**, *61*, 060410.
[3] G. C. Righini, J. Krzak, A. Lukowiak, G. Macrelli, S. Varas, M. Ferrari, *Opt. Mater.* **2021**, *115*, 111011.
[4] L. Li, H. Lin, S. Qiao, Y. Zou, S. Danto, K. Richardson, J. D. Musgraves, N. Lu, J. Hu, *Nat. Photonics* **2014**, *8*, 643.
[5] S. Kim, *Micromachines* **2019**, *10*, 267.
[6] X. Zeng, H. Jiang, *J. Microelectromech. Syst.* **2011**, *20*, 6.
[7] H. Wu, Y. Tian, H. Luo, H. Zhu, Y. Duan, Y. A. Huang, *Adv. Mater. Technol.* **2020**, *5*, 2000093.
[8] S. I. Rich, Z. Jiang, K. Fukuda, T. Someya, *Mater. Horiz.* **2021**, *8*, 1926.
[9] A. Purvis, R. McWilliam, S. Johnson, N. L. Seed, G. L. Williams, A. Maiden, P. Ivey, *J. Micro/Nanolithography, MEMS, MOEMS* **2007**, *6*, 043015.</bib
[10] H. Cai, Q. Meng, H. Ding, K. Zhang, Y. Lin, W. Ren, X. Yu, Y. Wu, G. Zhang, M. Li, N. Pan, Z. Qi, Y. Tian, Y. Luo, X. Wang, *ACS Nano* **2018**, *12*, 9626.
[11] S. Aksu, M. Huang, A. Artar, A. A. Yanik, S. Selvarasah, M. R. Dokmeci, H. Altug, *Adv. Mater.* **2011**, *23*, 4422.
[12] J. Liu, L. Xiao, Z. Rao, B. Dong, Z. Yin, Y. Huang, J. Liu, L. Xiao, Z. Rao, B. Dong, Z. Yin, Y. A. Huang, *Adv. Mater. Technol.* **2018**, *3*, 1800155.
[13] D. Espalin, D. W. Muse, E. MacDonald, R. B. Wicker, *Int. J. Adv. Manuf. Technol.* **2014**, *72*, 963.
[14] J. Yeo, S. Hong, M. Wanit, H. W. Kang, D. Lee, C. P. Grigoropoulos, H. J. Sung, S. H. Ko, *Adv. Funct. Mater.* **2013**, *23*, 3316.
[15] Z. Yan, M. Han, Y. Yang, K. Nan, H. Luan, Y. Luo, Y. Zhang, Y. Huang, J. A. Rogers, *Extreme Mech. Lett.* **2017**, *11*, 96.
[16] J. Ai, Q. Du, Z. Qin, J. Liu, X. Zeng, *Opt. Express* **2018**, *26*, 20965.
[17] D. Radtke, U. D. Zeitner, *Opt. Express* **2007**, *15*, 1167.
[18] Y. G. Kim, H. G. Rhee, Y. S. Ghim, *Int. J. Adv. Manuf. Technol.* **2021**, *114*, 1497.
[19] V. Harinarayana, Y. C. Shin, *Opt. Laser Technol.* **2021**, *142*, 107180.
[20] M. Carlotti, V. Mattoli, *Small* **2019**, *15*, 1902687.
[21] O. Tricinci, T. Terencio, B. Mazzolai, N. M. Pugno, F. Greco, V. Mattoli, *ACS Appl. Mater. Interfaces* **2015**, *7*, 25560.
[22] Y. Wang, Y. Du, J. Deng, Z. Wang, *Colloids Surfaces A* **2019**, *562*, 321.
[23] C. Liao, K. Yang, J. Wang, Z. Bai, Z. Gan, Y. Wang, *IEEE Photonics Technol. Lett.* **2019**, *31*, 971.
[24] P. I. Dietrich, M. Blaicher, I. Reuter, M. Billah, T. Hoose, A. Hofmann, C. Caer, R. Dangel, B. Offrein, U. Troppenz, M. Moehrle, W. Freude, C. Koos, *Nat. Photonics* **2018**, *12*, 241.
[25] C. Liberale, G. Cojoc, P. Candeloro, G. Das, F. Gentile, F. De Angelis, E. Di Fabrizio, *IEEE Photonics Technol. Lett.* **2010**, *22*, 474.
[26] C. Xiong, C. Liao, Z. Li, K. Yang, M. Zhu, Y. Zhao, Y. Wang, *Front. Mater.* **2020**, *7*, 369.
[27] R. A. Nawrocki, R. A. Nawrocki, *Adv. Funct. Mater.* **2019**, *29*, 1906908.
[28] J. Barsotti, A. G. Rapidis, I. Hirata, F. Greco, F. Cacialli, V. Mattoli, *Adv. Electron. Mater.* **2021**, *7*, 2001145.
[29] Y. Qi, N. T. Jafferis, K. Lyons, C. M. Lee, H. Ahmad, M. C. McAlpine, *Nano Lett.* **2010**, *10*, 524.
[30] H. S. Kim, C. R. Lee, J. H. Im, K. B. Lee, T. Moehl, A. Marchioro, S. J. Moon, R. Humphry-Baker, J. H. Yum, J. E. Moser, M. Grätzel, N. G. Park, *Sci. Rep.* **2012**, *2*, 591.
[31] M. C. Mcalpine, H. Ahmad, D. Wang, J. R. Heath, *Nat. Mater.* **2007**, *6*, 379.
[32] R. C. Webb, A. P. Bonifas, A. Behnaz, Y. Zhang, K. J. Yu, H. Cheng, M. Shi, Z. Bian, Z. Liu, Y. S. Kim, W. H. Yeo, J. S. Park, J. Song, Y. Li, Y. Huang, A. M. Gorbach, J. A. Rogers, *Nat. Mater.* **2013**, *12*, 938.
[33] J. J. S. Norton, D. S. Lee, J. W. Lee, W. Lee, O. Kwon, P. Won, S. Y. Jung, H. Cheng, J. W. Jeong, A. Akce, S. Umunna, I. Na, Y. H. Kwon, X. Q. Wang, Z. J. Liu, U. Paik, Y. Huang, T. Bretl, W. H. Yeo, J. A. Rogers, Z. Bao, *Proc. Natl. Acad. Sci. USA* **2015**, *112*, 3920.
[34] K. Autumn, Y. A. Liang, S. T. Hsieh, W. Zesch, W. P. Chan, T. W. Kenny, R. Fearing, R. J. Full, *Nature* **2000**, *405*, 681.
[35] D. H. Kim, J. Viventi, J. J. Amsden, J. Xiao, L. Vigeland, Y. S. Kim, J. A. Blanco, B. Panilaitis, E. S. Frechette, D. Contreras, D. L. Kaplan, F. G. Omenetto, Y. Huang, K. C. Hwang, M. R. Zakin, B. Litt, J. A. Rogers, *Nat. Mater.* **2010**, *9*, 511.
[36] G. Zabow, *Science* **2022**, *378*, 894.
[37] M. Kaltenbrunner, T. Sekitani, J. Reeder, T. Yokota, K. Kuribara, T. Tokuhara, M. Drack, R. Schwödiauer, I. Graz, S. Bauer-Gogonea, S. Bauer, T. Someya, *Nature* **2013**, *499*, 458.
[38] J. A. Rogers, M. G. Lagally, R. G. Nuzzo, *Nature* **2011**, *477*, 45.
[39] R. Vendamme, S. Y. Onoue, A. Nakao, T. Kunitake, *Nat. Mater.* **2006**, *5*, 494.
[40] C. Jiang, S. Markutsya, Y. Pikus, V. V. Tsukruk, *Nat. Mater.* **2004**, *3*, 721.
[41] T. Fujie, L. Ricotti, A. Desii, A. Menciassi, P. Dario, V. Mattoli, *Langmuir* **2011**, *27*, 13173.
[42] T. Fujie, A. Desii, L. Ventrelli, B. Mazzolai, V. Mattoli, *Biomed. Microdevices* **2012**, *14*, 1069.
[43] X. Liu, X. Lu, R. Chuai, C. Shi, C. Suo, *Sens. Actuators A* **2009**, *154*, 42.
[44] F. A. Viola, J. Barsotti, F. Melloni, G. Lanzani, Y. H. Kim, V. Mattoli, M. Caironi, *Nat. Commun.* **2021**, *12*, 5842.
[45] J. Barsotti, I. Hirata, F. Pignatelli, M. Caironi, F. Greco, V. Mattoli, *Adv. Electron. Mater.* **2018**, *4*, 1800215.
[46] Z. Yan, D. Xu, Z. Lin, P. Wang, B. Cao, H. Ren, F. Song, C. Wan, L. Wang, J. Zhou, X. Zhao, J. Chen, Y. Huang, X. Duan, *Science* **2022**, *375*, 852.
[47] A. Ottomaniello, P. Vezio, O. Tricinci, F. M. Den Hoed, P. Dean, A. Tredicucci, V. Mattoli, *Nanophotonics* **2023**, https://doi.org/10.1515/nanoph-2022-0667.
[48] S. H. Baxamusa, M. Stadermann, C. Aracne-Ruddle, A. J. Nelson, M. Chea, S. Li, K. Youngblood, T. I. Suratwala, *Langmuir* **2014**, *30*, 5126.
[49] G. L. Esparza, M. Kodur, A. X. Chen, B. Wang, J. A. Bunch, J. Cramlet, R. Runser, D. P. Fenning, D. J. Lipomi, *Adv. Mater.* **2023**, 2207798, https://doi.org/10.1002/adma.202207798.
[50] K. Yamagishi, S. Takeoka, T. Fujie, *Biomater. Sci.* **2019**, *7*, 520.
[51] J. B. Fortin, T.-M. Lu, *Chemical Vapor Deposition Polymerization*, Springer, USA **2004**.